Applied Catalysis A: General 453 (2013) 391–402

Contents lists available at SciVerse ScienceDirect

Applied Catalysis A: General

journal homepage: www.elsevier.com/locate/apcata

Influence of the synthesis conditions on the physicochemical properties and acidity of Al-MCM-41 as catalysts for the cyclohexanone oxime rearrangement

Eliana G. Vaschetto[a,c], Gustavo A. Monti[b,c], Eduardo R. Herrero[a], Sandra G. Casuscelli[a,c], Griselda A. Eimer[a,c,*]

[a] CITeQ-Universidad Tecnológica Nacional-Facultad Regional Córdoba, Maestro López esq. Cruz Roja Argentina, 5016 Córdoba, Argentina
[b] FaMAF-Universidad Nacional de Córdoba, Córdoba, Argentina
[c] CONICET, Argentina

ARTICLE INFO

Article history:
Received 17 October 2012
Received in revised form 5 December 2012
Accepted 9 December 2012
Available online 26 December 2012

Keywords:
Mesoporous materials
Al-MCM-41
Synthesis time
Gel stirring
ξ-Caprolactam

ABSTRACT

Al-containing mesoporous catalysts with MCM-41 structure and high surface area have been successfully prepared by direct hydrothermal synthesis. Various characterization techniques including XRD, N_2 adsorption, ICP-OES, NMR, FT-IR and adsorption of pyridine coupled to FT-IR spectroscopy were employed. A detailed study about the relationships existing between the different synthesis parameters, the physico-chemical properties, the acid behavior and the catalytic performance is presented in this contribution. We have suggested that the active sites for the Beckmann rearrangement of cyclohexanone oxime are nest silanols (at structural defects) of very weak Brønsted acid character, which is associated with the introduction of Al into the mesoporous framework. In all the cases, employing soft reaction conditions, we have obtained selectivity to caprolactam of 100%. Finally, a Si/Al initial molar ratio of 20, a stirring of synthesis gel for 7 h and a hydrothermal treatment of 6 days seem to be the optimum synthesis conditions to obtain the highest framework Al incorporation, more abundant weak acid sites (silanol nests) and maximum yield for ξ-caprolactam.

1. Introduction

The preparation and engineering of nanostructured porous silicate materials are one of the areas that will contribute the most to scientific and technological development along the 21st century.

Particularly, the MCM-41 molecular sieve, member of the family of mesoporous silica compounds M41S [1–8], has allowed developing applicable catalysts in many industrial processes. Features such as an hexagonal packed array of unidirectional mesopores (between 2 and 10 nm) with narrow pore size distribution, highly ordered structure, high surface area (up to 1000 m^2/g) and high specific pore volume (up to 1.3 ml/g) are mainly responsible for its high adsorption capacity even of bulky molecules. Meanwhile, the catalytic properties of these materials rely on the presence of active sites in their frameworks. In fact, since the first reports of these structures [3,4], numerous studies have been performed aiming to modify the pure siliceous MCM-41 in order to increase its potential applicability. Thus, the incorporation of aluminum within the silica framework has been implemented in order to increase the acidity, ion exchange capacity and specific catalytic activity [9–11]. In this respect, it has been shown that aluminum can be successfully incorporated into tetrahedral positions of the MCM-41 framework through direct hydrothermal synthesis [12,13]. This porous structure and its specific catalytic behavior can be tailored to a certain extent by controlling the synthesis parameters such as surfactant/Si ratio, surfactant nature, metal loading, stirring time of the synthesis gel, hydrothermal treatment time, temperature, etc. In particular, since the rates of polymerization of the silicium and aluminum species are different, the hydrothermal synthesis time as well as the stirring of the synthesis gel must be key parameters that can affect not only the textural properties but also the present metallic species and acidity of the final solid. On the other hand, given its considerably weak acidity and large pores system, this type of mesoporous sieves Al-MCM-41 has potential applications as catalysts in processes requiring moderate acidity and involving bulky molecules. Thus, considering these characteristic properties, the applicability of these catalysts has been studied in the Beckmann rearrangement reaction of the cyclohexanone oxime (CHO) to ξ-caprolactam (ξ-C) [14–20]. ξ-C is an important intermediate for the manufacture of synthetic fibers and engineering

* Corresponding author at: Maestro López esq. Cruz Roja Argentina, Ciudad Universitaria, 5016 Córdoba, Argentina. Tel.: +54 0351 4690585; fax: +54 0351 4690585.
E-mail addresses: geimer@scdt.frc.utn.edu.ar, griseeimer@yahoo.com.ar (G.A. Eimer).

0926-860X/$ – see front matter © 2012 Elsevier B.V. All rights reserved.
http://dx.doi.org/10.1016/j.apcata.2012.12.016

plastics, being a key starting material for the manufacture of Nylon 6. The classical process for the commercial production of caprolactam involves the cyclohexanone oximation and the liquid phase Beckmann rearrangement route, which is highly selective but ecologically and economically questionable. This process has several disadvantages such as the production of large amounts of low value ammonium sulfate as a waste and the corrosion and environmental pollution caused by the use of concentrated sulfuric acid as a homogeneous catalyst [21–23]. For this reason, more efficient, economical and environmentally compatible paths for the production of ξ-caprolactam are required. In this sense, several research groups have attempted to carry out the Beckmann rearrangement in the vapor phase using acid solid catalysts [14–17,21–44]. Recently, Ichihashi and Sato et al. [45,46] have developed a new process for the vapor phase Beckmann rearrangement of cyclohexanone oxime using a silica zeolite which has made possible the industrial production of caprolactam without producing any ammonium sulfate. Anyway, research on this field continues to be intense and, among the solid catalysts investigated, the Al-MCM-41 materials appear as very interesting. On the other hand, considerable attention has been focused on the type of catalytically active sites in the Beckman rearrangement and the relationship between the selectivity for caprolactam and the acidity. In the past years, it has been reported that moderate or strong Brønsted acid sites promote the formation of ξ-caprolactam while SiOH groups catalyze the formation of by-products [14,15,47,48]. In this sense, Chaudhari et al. [14] and Forni et al. [15] claim that the formation of caprolactam (rearrangement) is mainly favored by moderate acid centers present on Al-MCM-41 in their H-forms, which is deeply dependent of the framework aluminum content. On the contrary, many researchers have noticed that only weak or even extremely weak Brønsted acid sites, such as hydrogen bonded hydroxyls at framework defect sites (vicinal silanol groups or silanol nests), can be effective for the Beckmann rearrangement [22,43,44,49–54] while strong acid sites accelerate the formation of by-products [55,56]. Thus, Herrero et al. [44] stated that the weak Brønsted acidity associated with SiOH groups (external, in cavities and structural defects), in wide-pore zeolites and non-zeolitic materials, increases the caprolactam yield. In addition, Holderich et al. [54] reported that silanol nests with very weak acidity generated on MFI zeolites by treating with ammonia are the most favorable sites for the oxime rearrangement. Then, they observed that, on a [Al]-Beta zeolite, the vicinal hydrogen bonded hydroxyls also showed a favorable strength for this rearrangement [52]. Moreover, these authors suggested that a high calcination temperature of the material can produce (besides the loss of active hydroxyls) alumina which could block some active sites. In addition, Ichihashi and Sato et al. [45,46] attributed the high selectivity and activity for the vapor phase Beckmann rearrangement on a MFI-type zeolite, composed exclusively of silica, to the acid nest silanols located close to their pore mouths. Recently Zhang et al. [17] investigated the modification of Al-MCM-41 with P in order to generate more acid sites and improve the selectivity to caprolactam. From all these reports it can be inferred that the nature and acid strength of the active sites necessary for the vapor-phase Beckmann rearrangement of the cyclohexanone oxime are not clear yet and more research is required. In order to contribute to the understanding of the nature of the active sites in the Beckmann rearrangement reaction to obtain ξ-Caprolactam, in this paper we develop catalysts of the type Al-MCM-41, seeking the substitution of Si by Al into the structure. The influence of the Si/Al molar ratio and the stirring time in the synthesis gel as well as the hydrothermal treatment time on the physicochemical properties has been studied. Moreover, the introduction of aluminum into the framework and the acidity (nature and strength of acid sites) of the final solids were analyzed in relation to the catalytic performance.

2. Experimental

2.1. Synthesis

The mesoporous materials (Al-MCM-41) were prepared by hydrothermal synthesis using cetyltrimethylammonium bromide (CTABr, Merck, 99%) as template and tetraethoxysilane (TEOS, Aldrich 98%) as silicon source. Sodium hydroxide (NaOH, Cicarelli) aqueous solution 2 M was used for hydrolysis and pH adjustment, and sodium aluminate ($NaAlO_2$, Johnson Matthey) was used as source of aluminum. The catalysts were synthesized from a synthesis gel of molar composition: NaOH/Si = 0.50, CTABr/Si = 0.12, H_2O/Si = 132 and Si/Al = 20 or 60. In a typical synthesis, CTABr was dissolved in H_2O–NaOH solution and after heating (35–40 °C) to dissolve the surfactant, the TEOS was added and stirred for 30 min. The Al source was added and the synthesis gel was stirred at room temperature for 4–12 h. Then, this resulting gel was hydrothermal treated at 100 °C in a Teflon-lined stainless-steel autoclave under autogeneous pressure for 0–8 days (0 days corresponds to the material without hydrothermal treatment). The final solid was filtered, washed with distilled water and dried at 60 °C overnight. To remove the template, the samples were heated (heating rate of 2 °C/min) under N_2 flow up to 500 °C and kept at this temperature for 6 h; they were then calcined at 500 °C under air flow for 6 h. The samples were named as Al-M(*x*)*y*-*z*, where "*x*" is the Si/Al initial molar ratio, "*y*" is the time of hydrothermal treatment and "*z*" is the stirring time of the synthesis gel in h. For comparison, analogous aluminum-free MCM-41 samples were synthesized and named as Si-M-*y*-*z*.

2.2. Characterization

The X-ray diffraction (XRD) patterns were recorded in air at room temperature on a Philips PW 3830 diffractometer with Cu Kα radiation (λ = 1.5418 Å) in the range of 2θ from 1.5° to 7°. The interplanar distance ($d(1\,0\,0)$) was estimated using the position of the first X-ray diffraction line. The lattice parameter (a_0) of the hexagonal unit cell was calculated from the equation $a_0 = (2/\sqrt{3})d(1\,0\,0)$. Specific surface areas were measured using a Pulse Chemisorb equipment by single point at $P/P_0 = 0.3$ through the BET method. The samples were previously heated for 1 h at 300 °C under N_2 flow.

The Al content was determined by inductively coupled plasma optical emission spectroscopy (ICP-OES), using a VISTA-MPC CCD Simultaneos ICP-OES-VARIAN.

The solid state nuclear magnetic resonance (NMR) spectra were conducted on a Bruker Avance II 300 spectrometer operating at 78.2 MHz for ^{27}Al. The sample was spun at the magic angle at a rate of 5 kHz. Experiments were carried out at ambient probe temperature. The ^{27}Al spectrum was recorded using direct polarization with pulses of 1 μs duration and a relaxation delay of 2 s. Aluminum chemical shifts are quoted with respect to 1 M aluminum nitrate solution. Infrared analysis of the samples was recorded on a JASCO 5300 FT-IR spectrometer. The FT-IR spectra in the lattice vibration region were performed using the KBr 0.05% wafer technique. In addition, in order to evaluate the strength and type of acid sites, FT-IR spectral measurements of pyridine adsorption on the samples were also performed through the following procedure. Self-supported wafers of the samples (~20 mg and 13 mm of diameter) were prepared, placed in a thermostatized cell with CaF_2 windows connected to a vacuum line and evacuated for 7 h at 400 °C under a dynamic vacuum; residual pressure was smaller than 10^{-3} Pa. After cooling to room temperature, the spectrum of each sample was recorded (background spectrum). Afterwards the background spectrum was recorded, the solid wafer was exposed to pyridine vapors (Sintorgan, 99% purity) until saturate the system to 46 mm Hg at room temperature; the contact time at this pressure was 12 h. After an IR spectrum of the adsorbed pyridine at

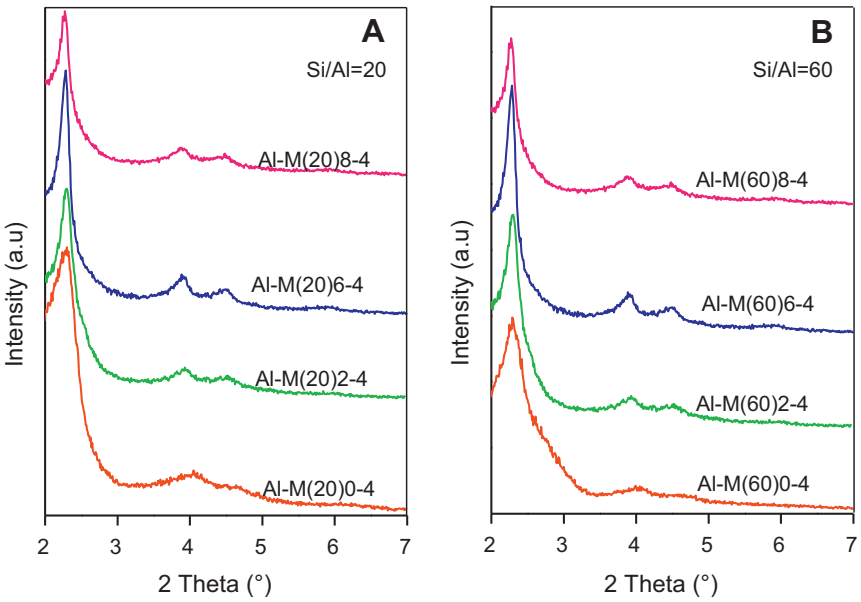

Fig. 1. XRD patterns of samples synthesized by stirring the synthesis gel for 4 h, with different hydrothermal treatment times, and Si/Al molar ratios (A) 20 and (B) 60.

room temperature was recorded, the subsequent IR spectra were obtained following the pyridine desorption by evacuation for 1 h at 25, 50, 100 and 200 °C. Finally, the difference spectrum for each sample was obtained by subtracting the background recorded previously.

2.3. Catalytic reactions

The catalytic reactions were carried out in a down flow fixed bed tubular glass reactor (i.d. = 8 mm and 35 cm length) at atmospheric pressure using 0.2 g of the catalyst. The reactor was placed inside a temperature controlled vertical furnace (320 °C). A solution of 10 wt% CHO in 1-hexanol was fed using a syringe pump (5.6 ml/min). CHO employed was 97% pure (Fluka). The contact time (W/F = 40 g h/mol) refers to the weight of catalyst (g) over the feed rate of CHO (mol/h). Nitrogen was used as the carrier gas (30 ml/min). The reaction products were collected in a receiver after cooling with ice cold water. The samples were analyzed using a Perkin Elmer gas chromatograph (Clarus 500) with a capillary column (ZB-1, 30 m × 0.53 mm i.d.) and a flame ionization detector (FID). The product identification was done by GC–MS (Perkin Elmer – clarus 560S) with a capillary column (E-5 30 m × 0.53 mm i.d.). Also the reaction products were analyzed by comparison with chromatographic standards.

The conversion was expressed in moles % and the yields calculated as: cyclohexanone oxime conversion × selectivity to reaction products/100.

3. Results and discussion

Table 1 summarizes the different synthesis conditions and physicochemical properties for the more representative samples prepared in this study. Fig. 1 shows the XRD patterns of the samples with initial Si/Al molar ratios = 20 and 60, obtained by stirring the reaction mixture for 4 h followed by different times of hydrothermal treatment (0–8 days). All of the patterns exhibit a main (1 0 0) peak and two weak reflections ascribed to (1 1 0) and (2 0 0), which is typical of highly ordered MCM-41 structures and consistent with the high surface area values obtained (above 1000 m^2/g). As it can be observed in both cases (Si/Al ratios = 20 and 60), even though the mesostructure was formed without thermal treatment, a notable improvement of the original structure was achieved when the samples were hydrothermal treated. Thus, the synthesis time has a considerable effect on the structural regularity. This is shown in Fig. 2 by evaluating the structural ordering degree of each sample in comparison to a sample arbitrary taken as reference with 100% ordering (Al-M(60)6-4) [57,58]. For both Si/Al ratios (20 and 60), a hydrothermal treatment time of 6 days appears optimum to obtain the higher long-range structural ordering. Then, a longer time appears to induce some disorder in the structure which can be also correlated with a decrease in the surface area observed (Table 1). These results are in agreement with some previous reports [57–59]. On the other hand, although all the samples exhibit high areas, those prepared with the lower Si/Al ratio showed relative areas slightly lower for the same times of stirring and hydrothermal treatment; this fact is attributed to a slight lowering of the lattice order degree associated with the higher Al incorporation. In addition, Fig. 3 shows the XRD patterns of the samples hydrothermal synthesized for 6 days with Si/Al molar ratios = 20 and 60, where the stirring time of synthesis gel was modified (4–12 h). As it can be seen, the high structural regularity of the samples is not notably affected by this synthesis variable though the surface area values seem to be slightly decreased when the stirring of gel is longer (Table 1). Finally, the increase in the parameter a_0 for all of the

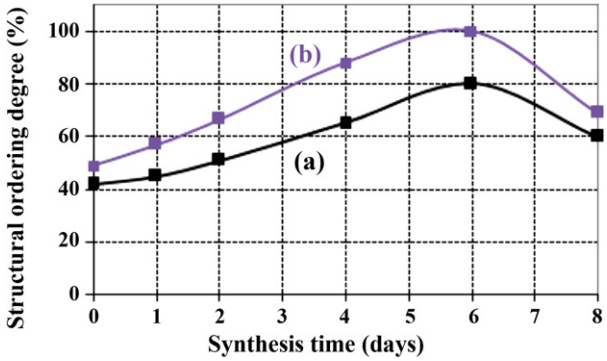

Fig. 2. Effect of synthesis time on the structural ordering degree of samples synthesized with Si/Al molar ratio in the synthesis gel of (a) 20 and (b) 60.

Table 1
Synthesis parameters and the physical properties of the synthesized solids.

Sample	Si/Al[a] (initial molar ratio)	Hydrothermal treatment (days)	Stirring of the synthesis gel (h)	a_0[b] (nm)	Area (m^2/g)
Al-M(20)0-4	20	0	4	4.45	1275
Al-M(20)2-4	20	2	4	4.49	1364
Al-M(20)6-4	20	6	4	4.45	1293
Al-M(20)6-7	20	6	7	4.45	1242
Al-M(20)6-12	20	6	12	4.47	1188
Al-M(20)8-4	20	8	4	4.47	1131
Al-M(60)0-4	60	0	4	4.45	1387
Al-M(60)2-4	60	2	4	4.41	1414
Al-M(60)6-4	60	6	4	4.32	1398
Al-M(60)6-7	60	6	7	4.45	1277
Al-M(60)6-12	60	6	12	4.47	1161
Al-M(60)8-4	60	8	4	4.47	1172
Si-M-6-4	–	6	4	4.20	1180
Si-M-6-7	–	6	7	4.22	1182

[a] In the synthesis gel.
[b] $a_0 = (2/\sqrt{3})d_{100}$.

samples containing Al with respect to the purely siliceous sample is a hint of the incorporation of Al into the framework.

The NMR technique is widely used to characterize the coordination state of Al atoms in mesoporous structures. ^{27}Al NMR measurements were conducted to distinguish between tetrahedral and octahedral aluminum coordination in order to establish the degree of aluminum substitution (tetrahedral sites) in the silica framework. All spectra for our samples (Figs. 4 and 5) exhibit a peak at 59 ± 2 ppm corresponding to tetrahedral coordinated aluminum into the framework and a peak at 0 ± 2 ppm attributed to the octahedral coordinated extraframework aluminum [12,13,16,19]. It is known that the extraframework Al species (aluminum oxide) can be formed intrinsically during the hydrothermal crystallization and/or by expelling from the structure (dealumination) during calcination. It should be also noted here that tricoordinated framework aluminum species in a distorted tetrahedral geometry, which exist in a metastable state, frequently appear as a broad hump overlapped with the Al_{Td} peak [60]. Although this signal could not be discerned in our NMR spectra its existence can not be discarded. Assuming that the amounts of the tetrahedral and octahedral aluminum are proportional to their respective resonance intensities, it is notable the predominance of extraframework aluminum in all of the calcined samples prepared here. However, it can be observed that the relative proportion of tetrahedral coordinated Al into the framework (Al_{Td} %), calculated from the integrated intensities of the NMR peaks and shown in Table 2, is higher for the samples synthesized with the lower Si/Al initial ratio. This suggests that, employing this synthesis method, the incorporation and stabilization of Al into the framework are more favorable for the higher amounts of metal. In addition, the wt% of tetrahedral Al in the samples (Al_{Td} wt%), calculated from the Al_{Td} % multiplied with the overall Al content (accurately determined by ICP-OES), is also shown in Table 2. Both the hydrothermal synthesis time and the stirring time appear as important parameters in order to achieve the incorporation of tetrahedral Al into the framework. Thus, as it can be seen in Fig. 4 and Table 2, for both Si/Al initial ratios, a hydrothermal treatment of 6 days is optimum to reach the maximum percentage of tetrahedral Al into the framework (Al_{Td} % and Al_{Td} wt%). A longer synthesis time (8 days) shows a decrease in the Al incorporation, which would be probably consistent with the decrease of structural ordering and surface area. In addition, as it is shown in Fig. 5 and Table 2, while for the Si/Al ratio = 60 a stirring of the gel for 4 h seems to be sufficient to allow the maximum Al_{Td} % and Al_{Td} wt%, a longer stirring time (7 h) is necessary in order to introduce the highest amount of

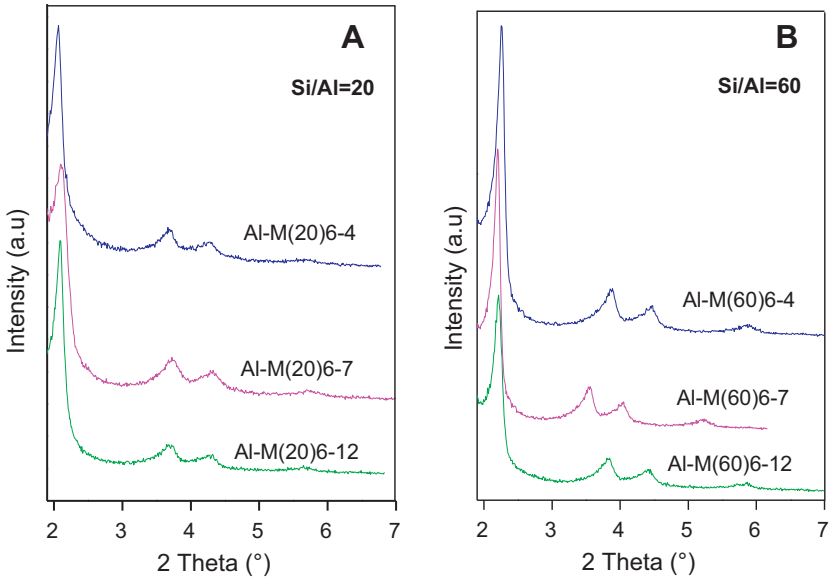

Fig. 3. XRD patterns of samples synthesized by hydrothermal treatment during 6 days with different stirring times and Si/Al molar ratios of (A) 20 and (B) 60.

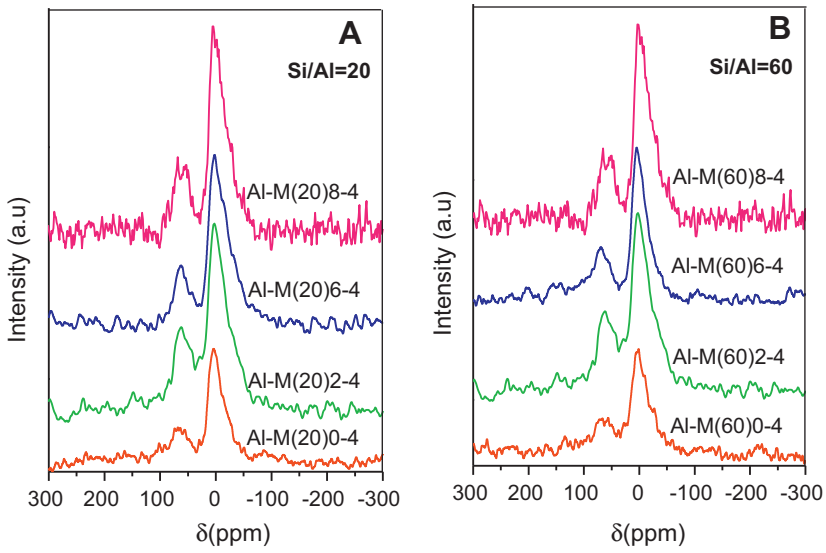

Fig. 4. ^{27}Al solid-state MAS NMR spectra of samples synthesized by stirring the synthesis gel for 4 h, with different hydrothermal treatment times, and Si/Al molar ratios (A) 20 and (B) 60.

tetrahedral coordinated Al into the framework (Al-M(20)6-7 sample). Finally, it is important to highlight here the very low content of residual sodium in all of the samples (lower 0.2 wt% for the Si/Al ratio = 20 and lower 0.07 wt% for Si/Al ratio = 60). Moreover, the molar ratio between the Na^+ and tetrahedral Al amounts is closed to one which suggests that the framework Al species would have mainly Na^+ as counter cations. The infrared spectra in the 400–1600 cm^{-1} range, named the fingerprint zone of the material, for the KBr-pelletized samples are shown in Figs. 6 and 7. Fig. 6 shows the spectra of the samples with Si/Al initial molar ratios = 20 and 60, obtained by stirring the synthesis gel for 4 h followed by hydrothermal treatment for different times; Fig. 7 shows the spectra of the samples hydrothermal synthesized for 6 days but stirring the gel during different times. The main bands described in the literature for MCM-41 are found in our samples, particularly the bands at around 1081 and 1243 cm^{-1} associated to internal and external asymmetric Si—O stretching modes, respectively, as well as the bands at 800 and 458 cm^{-1} assigned to symmetric stretching and tetrahedral bending of Si—O bonds, respectively [12,13,61,62]. Moreover, a strong band at 960 cm^{-1} is clearly visible in all of the spectra. For Ti-containing zeolites, a band at 960 cm^{-1} is believed to be a consequence of the stretching vibration of Si—O units bound to Ti atoms [63–66]. Several authors have assigned this band to the incorporation of heteroatoms such as Al or B into the framework of the mesoporous silica materials [22,23,62,67]. Thus, Palani et al. [62] attributed the presence of bands at 960–965 cm^{-1} to $Si—O^-M^+$ (where M = Al and Zn). However, caution is required in assigning this band since pure silica MCM-41 also exhibits such band around 960 cm^{-1} attributed to the Si—O stretching vibration in the Si—O—H groups at the defect sites present in the mesoporous structure [66]. Therefore, this band can be interpreted, in our samples, in terms of the overlapping of both Si—OH groups and Si—O—Al bonds vibrations. Anyway, when various metals are incorporated, the intensity of this band increases and this is generally considered to be a proof of the incorporation of the heteroatom into the framework [67]. In particular, Zhang et al. [68] claimed that the IR

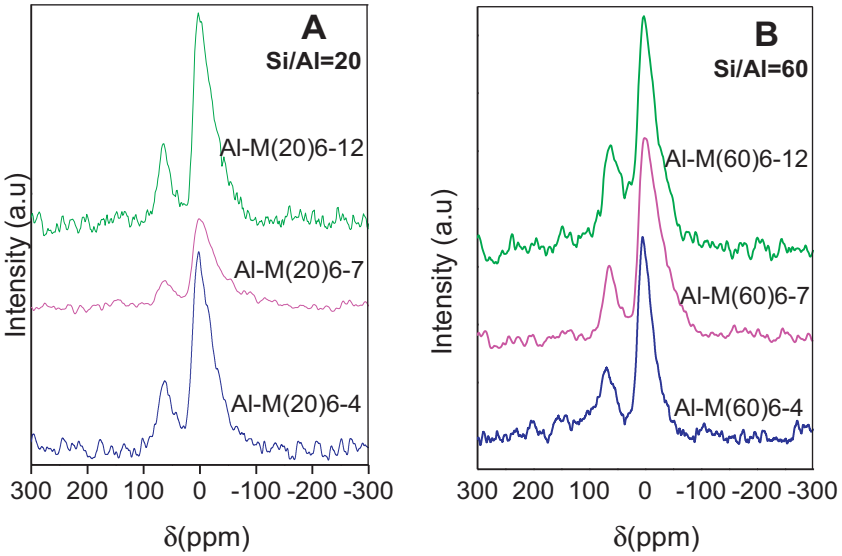

Fig. 5. ^{27}Al solid-state MAS NMR spectra of samples synthesized by hydrothermal treatment during 6 days, with different stirring times and Si/Al molar ratios (A) 20 and (B) 60.

Table 2
Chemical compositions, infrared data and ξ-C yield for the catalysts evaluated.

Sample	Al content (wt%)[a]	Al_{Td} (%)[b]	Al_{Td} (wt%)	A_{960}/A_{800}[c]	$A_{(1632)}$[d] (cm^{-1})	A_{1632}/A_{1447}[c]	ξ-C yield (mol%)[e]
Al-M(20)0-4	1.26	15.25	0.1921	0.78	0.19	0.083	6.10
Al-M(20)2-4	1.28	17.35	0.2221	1.25	0.68	0.298	17.00
Al-M(20)6-4	1.62	18.03	0.2921	1.57	1.21	0.535	36.80
Al-M(20)6-7	1.65	19.35	0.3192	2.04	1.35	0.592	60.43
Al-M(20)6-12	1.63	18.70	0.3048	1.84	1.30	0.571	54.20
Al-M(20)8-4	1.35	15.97	0.2156	1.05	0.27	0.118	10.60
Al-M(60)0-4	0.42	13.79	0.0579	0.75	0.16	0.059	5.00
Al-M(60)2-4	0.42	15.25	0.0641	1.18	0.50	0.185	16.10
Al-M(60)6-4	0.43	18.70	0.0804	1.54	1.00	0.363	36.00
Al-M(60)6-7	0.42	18.03	0.0757	1.48	0.91	0.336	30.91
Al-M(60)6-12	0.42	17.35	0.0728	1.45	0.79	0.292	22.43
Al-M(60)8-4	0.39	15.25	0.0594	0.81	0.25	0.092	7.43
Si-M-6-4	–	–	–	0.67	0.12	0.055	3.00
Si-M-6-7	–	–	–	0.68	0.13	0.057	3.12

[a] By ICP-OES.
[b] By NMR.
[c] Integrated absorbance ratio of IR bands.
[d] Integrated absorbance (cm^{-1}) of 1632 cm^{-1} IR band.
[e] Reaction conditions: TOS = 15 min, W/F = 40 g h/mol, temperature = 320 °C.

intensity at 960 cm^{-1} increased with increasing P content in MCM-41 materials as a consequence of the replacement of Si—O—H by Si—O—P. Nevertheless, considering the 960 cm^{-1} band as a further evidence of the Al incorporation in the material, we analyzed the variation of the relationship between the integrated absorbances of this IR band and that at 800 cm^{-1} ($\nu_{sy\ (Si-O-Si)}$) (A_{960}/A_{800}), in function of the different synthesis variables (Table 2). As it can be seen, for both Si/Al initial molar ratios, this relationship increases with the increase of the hydrothermal treatment time up to 6 days and then decreases. This fact would be indicating that a hydrothermal treatment of 6 days is optimum to reach the maximum concentration of Al incorporated into the framework of MCM-41 (Si—O—Al bonds), which is consistent with the NMR results. On the other hand, for the Si/Al ratio = 60, 4 h stirring the synthesis gel allows to achieve the highest value of the 960/800 cm^{-1} bands ratio, but in the case of the highest Al content, a longer time of stirring is necessary (7 h) to reach the higher Al incorporation. This is again according to the NMR results.

In order to detect the presence of silanol groups on the surface, Fig. 8 depicts the FTIR spectra in the hydroxyl range of the Al-M(20) samples (hydrothermally synthesized for 6 days after stirring the gel during different times) and of the purely siliceous analog. Before measurements, self-supported wafers of the samples were degassed at 400 °C for 7 h. It is known that there can be several types of surface silanol groups with different acidic properties: terminal, geminal, vicinal and nests [45,46,52,54,69–71]. All our spectra exhibited a broad and intense band that was attributed to hydrogen bonded hydroxyl groups [52,54,69,70]; this band could be separated into two contributions at about 3700 cm^{-1} and 3590–3600 cm^{-1} and subsequently fitted with two overlapping Gaussian peaks. According to the literature [45,46,52,54] these two contributions could be assigned to vicinal silanol groups and silanol nests, respectively, generated at framework defect sites probably due to the method used for catalyst preparation. In accordance with Hölderich et al. [52], the broadness can be explained by the stronger delocalization of the hydrogen bonded sites, because of the relative proximity of the hydroxyl groups in a silanol nest or even in vicinal silanols. At the same time, the shift of these bands to lower wavelength compared to that of the terminal silanol (around 3740 cm^{-1}, not found in our samples) also indicates the lateral interactions

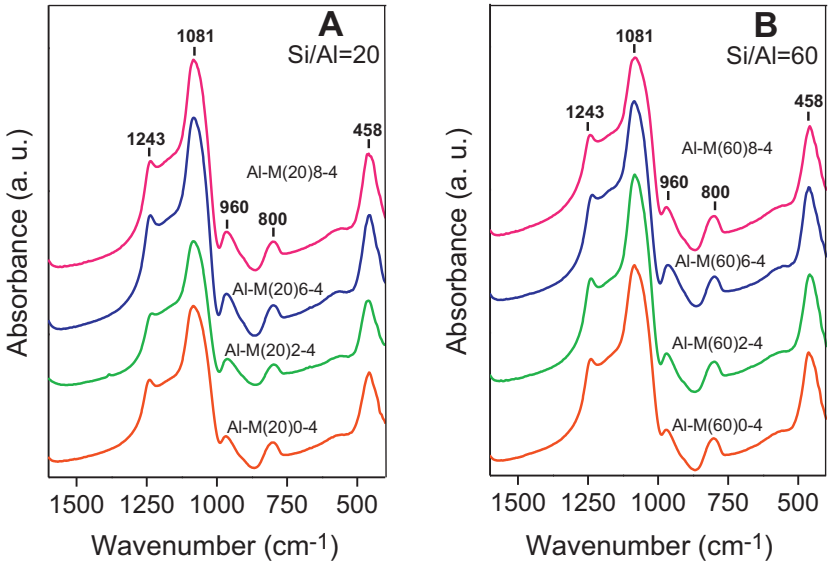

Fig. 6. FT-IR spectra in the 400–1600 cm^{-1} range of samples synthesized by stirring the synthesis gel for 4 h, with different hydrothermal treatment times, and Si/Al molar ratios (A) 20 and (B) 60.

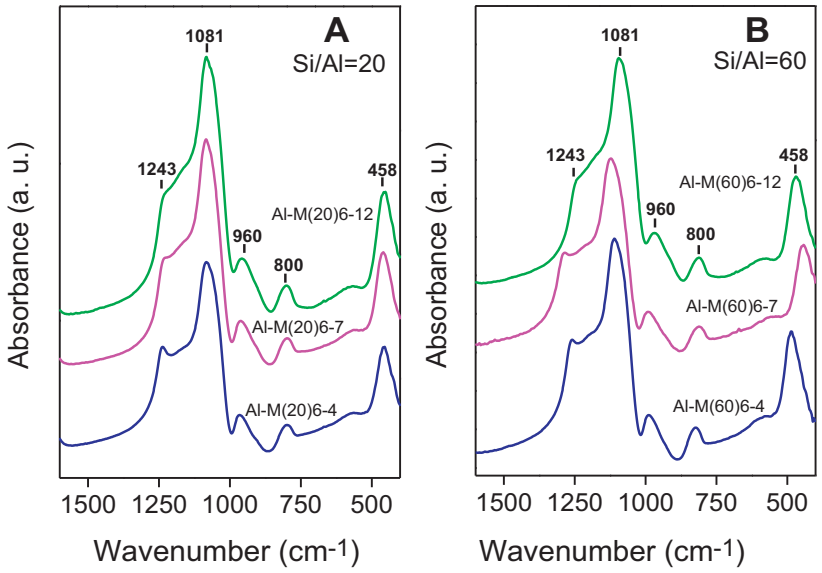

Fig. 7. FT-IR spectra in the 400–1600 cm^{-1} range of samples synthesized by hydrothermal treatment during 6 days, with different stirring times and Si/Al molar ratios (A) 20 and (B) 60.

of the silanol groups with each other through hydrogen bonds at the defect sites; these are expected to be more in samples having higher framework aluminum [70]. Thus, comparing the integrated absorbances of the two contributions for the different samples, it is possible to observe that even if the siliceous MCM-41 contains silanol nests, its relative proportion increases with increasing framework aluminum amount (see Fig. 8). Thus, the Al-M(20)6-7 sample, which has the maximum Al_{Td} % and Al_{Td} wt%, also shows the highest proportion of silanol nests. This fact is indicating that

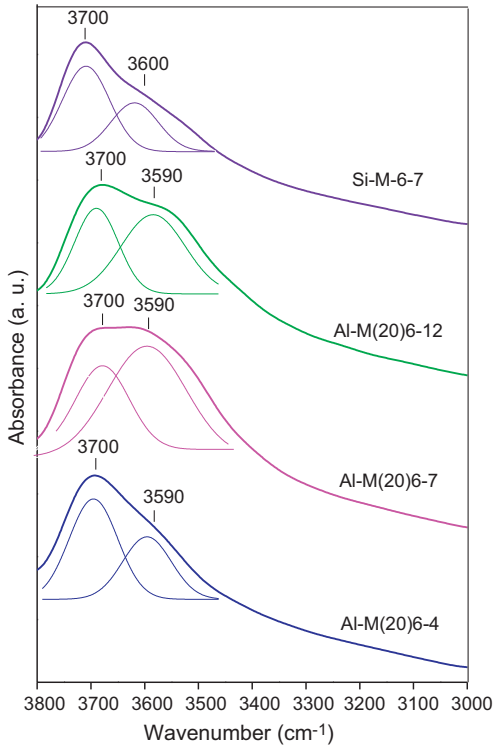

Fig. 8. FTIR spectra in the hydroxyl stretching region after degassing at 400 °C for Al-M(20) samples (hydrothermally synthesized for 6 days after stirring the gel during different times) and for the purely siliceous analog.

the incorporation of Al into the framework results in an increased formation of structural defects [69] leading to a higher proportion of silanol nests. In order to investigate the acidity of different silanol species, Sato et al. [46] studied and compared their deprotonation energies by means of molecular orbital calculation. They found that the ease of proton escape from silanol was in the order: nest, vicinal, geminal and terminal. This suggests that the nest silanol's acidity is the strongest of all silanols; thus the nest silanols can give a proton to a basic molecule easier than other silanols because the deprotonated species of nest silanols might be stabilized with the help of hydrogen bonding [45,46]. Likewise, the higher acidic character of the nest silanol is consistent with its lower vibrational frequency (lower O—H bond strength) and contrasts with higher frequencies for vicinal or terminal silanols Moreover, for our samples, the component assigned to nest silanol slightly shifts to a lower frequency (3590 cm^{-1}) (Fig. 8) in the Al modified samples compared with the siliceous sample. This could evidence a weakening of O—H bond and hence an enhanced acid character of the nest silanols as result of the incorporation of aluminum. Finally, it is notable that no bands corresponding to Brønsted acid sites, arising from isolated bridging Si(OH)Al hydroxyl groups, were found in this region of IR spectrum [69–71]. Despite the well documented mild acidity of Al-MCM-41 materials and the presence of tetrahedral Al in their structure, no significant evidence for the formation of bridging Si(OH)Al groups in the ordered mesoporous materials is provided in the literature. Occasionally, reported weak IR bands in the region of 3600 cm^{-1} [66,69,70] should probably be attributed to defects or impurities.

The chemisorption of pyridine followed by IR studies is usually a useful probe to detect the presence and nature of acid sites on a catalyst [73]. The pyridine, as basic molecule, can interact via the nitrogen lone-pair electrons with these acid sites, giving rise to characteristic bands. Information on the strength of Lewis and Brønsted acid sites can be obtained from pyridine thermodesorption. Fig. 9A and B shows the FT-IR spectra of the calcined sample Al-M(20)6-7 and the purely siliceous analog, respectively, recorded after the adsorption of pyridine at room temperature and after subsequent evacuation at 25, 50, 100 and 200 °C. Note that in order to make a semi quantitative and comparative analysis, all of the curves were affected by the wafer mass. It is known that pyridine can form hydrogen bonds with the silanol groups present in the structure whose hydroxyls are not capable to protonate pyridine. Thus, all our

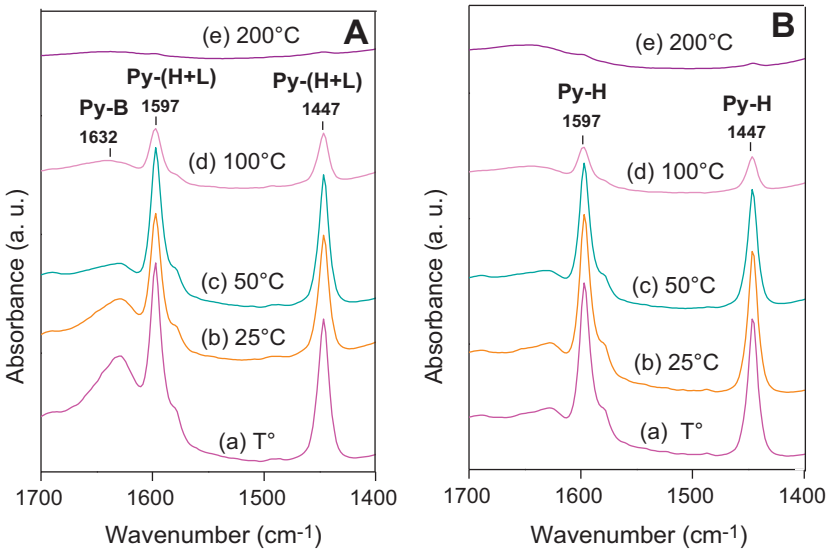

Fig. 9. FT-IR of pyridine adsorbed on the samples (A) Al-M(20)6-7 and (B) Si-M-6-7 at room temperature (a) and after subsequent evacuation at (b) 25, (c) 50, (d) 100 and (e) 200 °C.

samples show bands corresponding to silanol bonded pyridine at 1597 and 1447 cm^{-1} [23,69,70,72–76] which completely disappear upon evacuation at 200 °C. However, according to the literature and to our previous reports [23,69,70,72,73,75,77–79] the formation of a Lewis-type adduct with adsorbed pyridine is identified by IR absorption bands at about 1600–1620 and 1445–1455 cm^{-1}. As it can be observed in Fig. 9, upon evacuation at 100 °C, the integrated absorbances of the bands at 1597 and 1447 are slightly higher for the Al-MCM-41 sample (Fig. 9A) than for the purely siliceous material (Fig. 9B); this could evidence a contribution (overlapping these bands) from pyridine bonded to Lewis acid sites on Al-MCM-41 which are slightly stronger to retain the pyridine molecules until 100 °C. This Lewis acidity can be assumed to come, at least mainly, from extra-framework aluminum oxide (alumina) formed during calcination [70,77]. As it has been reported [80,81] the alumina only presents bands of pyridine bonded to Lewis acid sites. Nevertheless, it is important to note here that Katovic et al. [82] reported the formation of two different Lewis sites on Al-MCM-41 which were identified by CO adsorption coupled to FT-IR spectroscopy. Thus, they observed a strong signal due to extraframework Al sites and weak one assigned to $Al(OSi)_3$ species inside the framework [82]. These latter Lewis acid sites could be associated with the tricoordinated framework Al in a distorted tetrahedral geometry mentioned by Ma et al. [60]. We could not discern yet if these species contribute to the total Lewis acidity in our materials. Moreover, the presence of isolated sodium cations could also be contributing to this Lewis acidity. On the other hand, the presence of a band at 1632 cm^{-1}, which is remarkably more intense for the Al-MCM-41 sample, can be attributed to pyridine interacting with Brønsted sites from acid hydroxyls [71,78,83]. In this sense, Chen et al. [84] assigned this band to pyridine adsorbed on the hydroxyl ions. A relevant fact is the absence of the pyridinium ion band at about 1545 cm^{-1} arising from pyridine interacting with bridging Si(OH)Al hydroxyl groups [71,83]. This allows us to postulate that the OH groups giving rise to the 3590 cm^{-1} band (nest silanols with weak acid character) could be mainly involved in pyridine protonation

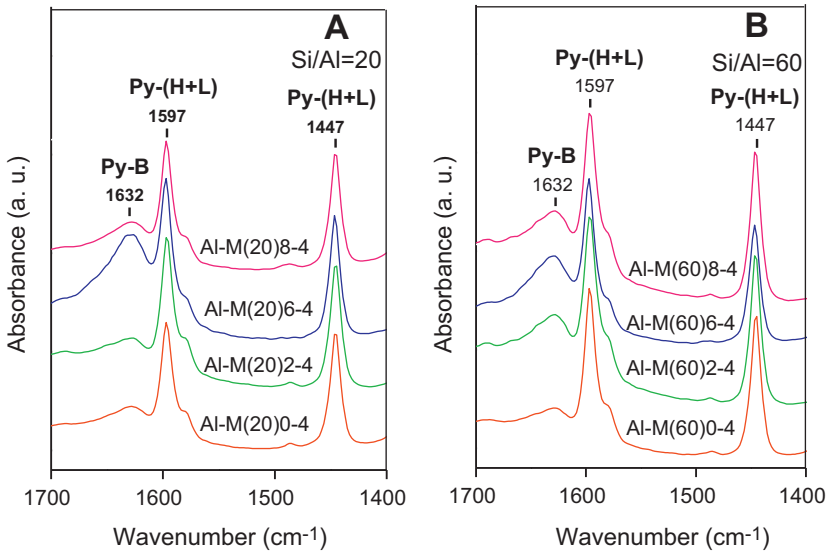

Fig. 10. FT-IR of pyridine adsorbed at room temperature on samples synthesized by stirring the synthesis gel for 4 h, with different hydrothermal treatment times, and Si/Al molar ratios (A) 20 and (B) 60.

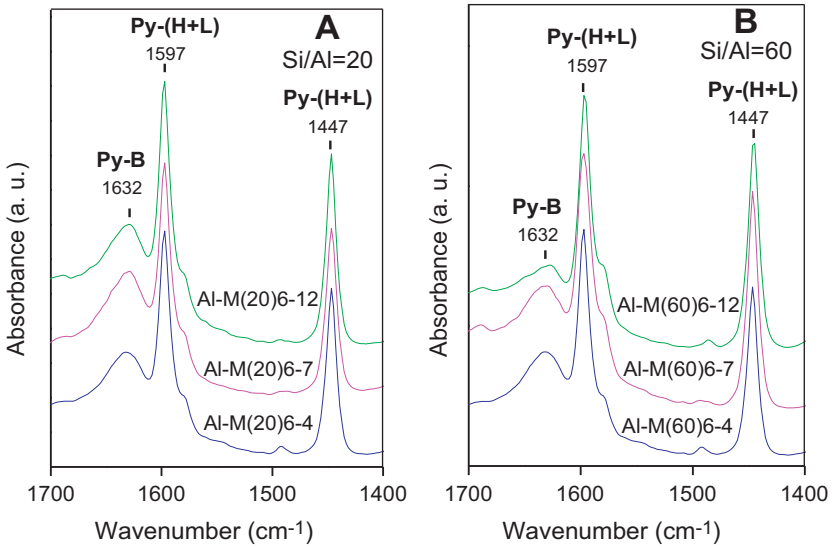

Fig. 11. FT-IR of pyridine adsorbed at room temperature on samples synthesized by hydrothermal treatment during 6 days, with different stirring times and Si/Al molar ratios (A) 20 and (B) 60.

on Al-MCM-41 samples [83]. Under evacuation at 50 °C the band at 1632 cm^{-1} tends to disappear, indicating that these Brønsted sites are of a very weak character. It should be noted that the pyridine desorption temperature is significantly lower than that for zeolites, which reflects the higher acidity of zeolites. In accordance with Refs. [71,82–85] we conclude that the weak Brønsted sites in our Al-MCM-41 materials are not due to bridging Al(OH)Si groups, which are commonly found in zeolites, but they would be mainly associated with surface acid SiOH groups such as the silanol nests observed in Fig. 8. It is noteworthy that although the siliceous sample possesses silanol nests, the same presents a very low intensity for the 1632 cm^{-1} band. Hence, it is possible suggest that the acidic properties of these silanol nests are most likely modified by the inductive effect of the Al present into the structure. Thus, changes in the electron density around Si due to charge unbalance, or differences in electronegativity or local structure deformation resulting from the introduction of Al into the vicinity of the hydroxyl carrying silicon may weaken the SiO—H bond in silanol nests, enhancing their acid strength. In this regard, Coles et al. [86] have shown that the insertion of aluminum species in mesoporous molecular sieves framework creates electrophilic cationic Al centers, which could contribute to weakening of SiO—H bond. Likewise, it is highly likely that the tricoordinated framework Al species, if they exist, produce strongly electroacceptor sites. Thereby, aluminum clearly influences silanol bond strengths and some of these may well give rise to Brønsted acidity; however, it is probable that only a very small proportion of the total silanol population exhibits Brønsted acidity. Fig. 10A and B shows the FT-IR spectra of adsorbed pyridine at room temperature on the samples with Si/Al initial molar ratios = 20 and 60, respectively, obtained by stirring the synthesis gel for 4 h followed by hydrothermal treatment for different times. Fig. 11A and B shows these spectra for the samples hydrothermally synthesized during 6 days but stirring the gel during different times. All of the above mentioned bands have been observed in these spectra. Taking into account that the bands at 1597 and 1447 cm^{-1} are interpreted in terms of the overlapping of both the hydrogen-bonded pyridine and a Lewis-type adduct, the main aim of showing these spectra is to draw attention to the intensity of the band at 1632 cm^{-1} (Brønsted acid silanols). Although these IR spectra cannot be regarded as being strictly quantitative, considering that the sample wafers had approximately the same surface density and that all of the measurements were affected by the wafer weight, a semi quantitative analysis is valid. Thus, the integrated absorbance (A_{1632}) of the 1632 cm^{-1} IR band (Brønsted acid silanols) as well as the ratio (A_{1632}/A_{1447}) between this and the integrated absorbance (A_{1447}) of the 1447 cm^{-1} band (Lewis sites and non-acid silanols), after pyridine absorption at room temperature, have been calculated to estimate the acid site density (Table 2). As it can be seen, all of the samples with higher Al content (Si/Al ratio = 20) present higher Brønsted acid silanol density (A_{1632}) than the corresponding ones synthesized with lower metal content (Si/Al ratio = 60). Moreover, considering the variation in the hydrothermal synthesis time, for both Si/Al ratios, the A_{1632} as well as the A_{1632}/A_{1447} ratio increased with increasing this variable up to 6 days and then markedly decreased (Fig. 10 and Table 2). This increase in the Brønsted acidity arising from acid silanols can be clearly associated with the higher presence of framework Al for 6 days of hydrothermal treatment, in agreement with the NMR results. With respect to the stirring time of gel, for the Si/Al ratio = 60 the Brønsted acid silanol density is only slightly affected by this variable, but in the case of the Si/Al ratio = 20, an increase in both the A_{1632} and the A_{1632}/A_{1447} ratio was observed by stirring the gel for 7 h (Fig. 11 and Table 2). Again, this maximum Brønsted acidity arising from acid silanols for the sample Al-M(20)6-7 is consistent with the higher proportion of framework Al. Finally, Fig. 12 illustrates the clear

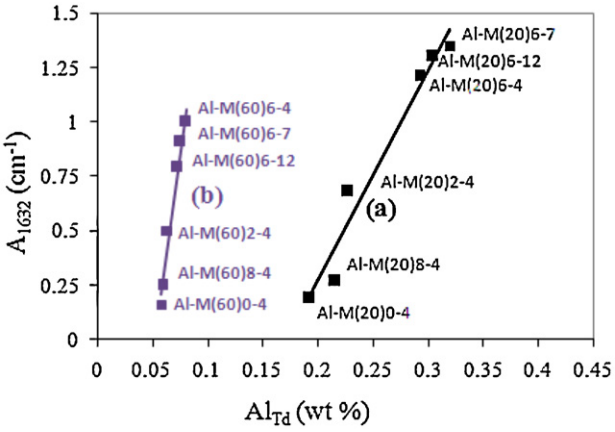

Fig. 12. Brønsted acid silanol density (A_{1632}) versus the concentration of framework Al (Al_{Td} wt%) for samples synthesized with Si/Al mol ratios of (a) 20 and (b) 60.

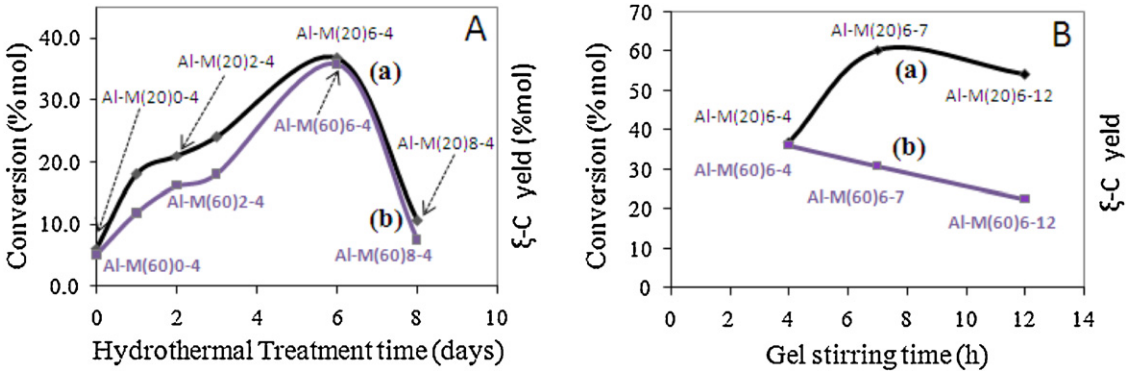

Fig. 13. CHO conversion and ξ-C yield versus: (A) hydrothermal treatment time for samples synthesized by stirring the gel for 4 h and Si/Al ratios of (a) 20 and (b) 60; (B) gel stirring time for samples synthesized by hydrothermal treatment during 6 days and Si/Al ratios of (a) 20 and (b) 60.

linear increase in the Brønsted acid silanol density (A_{1632}) when the concentration of Al incorporated into the framework was increased, under the different synthesis conditions. These results confirm that the introduction of Al into the mesoporous framework not only increases the proportion of silanol nests due to an increased formation of structural defects but also enhances their acid strength, generating thus Brønsted sites arising from acid SiOH groups. On the other hand, some authors [69,77] have found that the relative intensity of the bands assigned to pyridine bonded to hydrogen decreases as the Al incorporation increases leaving less number of non acidic silanol groups in the material. For our samples, a similar behavior in the integrated absorbances of these bands can be inferred when the Si/Al ratio decreases from 60 to 20 (Figs. 10 and 11). This fact is consistent with the vicinal silanols proportion (band at 3700 cm^{-1}) decreasing with increasing Al incorporation. However, as it was mentioned, the contribution from Lewis sites to the hydrogen-bonded pyridine bands cannot be discarded.

Table 2 shows the catalytic results for the vapor-phase Beckmann rearrangement reaction of the cyclohexanone oxime to ξ-caprolactam, at 320 °C and W/F = 40 g h/mol, over the more representative synthesized catalysts. It is known that the cyclohexanone oxime can be catalytically transformed to products of rearrangement, fragmentation and hydrolysis under different reaction conditions. We have chosen mild reaction conditions in order to obtain moderate conversion values with high ξ-caprolactam selectivity, that which allows us to establish the possible nature of the active sites in the rearrangement reaction. The influence of the synthesis conditions of material (hydrothermal treatment time and stirring time of the synthesis gel) on the catalytic performance for the Si/Al ratios = 20 and 60 are illustrated in Fig. 13. For both Si/Al ratios, the materials hydrothermal treated during 6 days exhibited the better catalytic performance (Fig. 13A). Meanwhile, a stirring of the gel for 7 h allowed to achieve the best catalytic result (conversion ~60%) for the catalyst with higher Al content (Si/Al ratio = 20) and 6 days of hydrothermal treatment (Fig. 13B). Then, as it is shown in Fig. 14, a linear relationship between the yield to ξ-caprolactam and the Brønsted acid silanols density (A_{1632}) on the catalysts was found for each variable analyzed. In addition, it is very interesting to note that the ξ-caprolactam selectivity was 100% on all our catalysts. Taking in mind that neither the Si-M sample (non-acid sites) nor alumina impregnated on the siliceous sample, tested by us, presented activity and that strong acid sites can accelerate the formation of by-products [55,56] we propose that the nest silanols with their very weak Brønsted acidity, which arises from the introduction of Al into the framework, are actually the active sites for the vapor-phase Beckmann rearrangement [45,46,54]. Thus, these hydroxyl groups (nest silanols) on the Al-MCM-41, synthesized by us, seem to have a favorable acid strength to give a proton to cyclohexanone oxime, playing an important role in the Beckmann rearrangement of the CHO with very high selectivity toward ξ-caprolactam. Although it is important to note that we have not found activity for the alumina, Heitmann et al. [52] have suggested that the presence of non active extra framework alumina can cause a blockage of catalytic active sites. To which extent this segregated alumina can contribute on the catalytic performance has not been found yet. Nevertheless, we think that, judging by thefinely

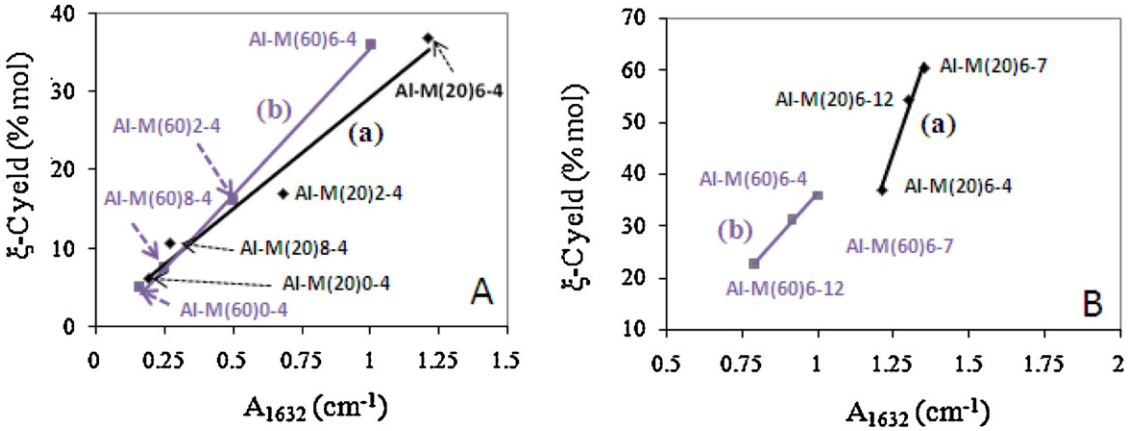

Fig. 14. ξ-C yield versus Brønsted acid silanol density (A_{1632}) for: (A) samples synthesized by stirring the synthesis gel for 4 h with different hydrothermal treatment times and Si/Al molar ratios of (a) 20 and (b) 60; (B) samples synthesized by hydrothermal treatment during 6 days with different stirring times and Si/Al molar ratios of (a) 20 and (b) 60.

dispersion of alumina on surface (not detected by XRD) and the results obtained, its interference on the activity of our catalysts should not be important. Finally, in order to verify the formation of coke, in one of our experiments the catalyst was recovered and heated at 500 °C. A negligible difference in the weight was determined. Therefore, it is evidence that under our reaction conditions the coke formation is insignificant.

Based on the above results, the optimum synthesis conditions which maximize the density of weak Brønsted acid silanols (active sites) hence the yield to ξ-caprolactam are: Si/Al initial ratio = 20, hydrothermal treatment time = 6 days and stirring time of initial gel = 7 h (Al-M(20)6-7 sample). Finally, although some authors have informed higher values of CHO conversion on Al-MCM-41 mesoporous catalysts under reaction conditions more severe in most cases (higher temperatures and *W*/*F*, harmful solvents) [14–17], nobody reported values of selectivity to ξ-caprolactam of 100%. Up to the moment we have achieved to understand the active site nature involved in the Beckmann rearrangement and have found the best synthesis conditions to maximize the amount of these sites. However, more detailed studies are necessary to optimize the reaction conditions in order to maximize the yield to ξ-caprolactam, which will be object for a next work.

4. Conclusions

Al-MCM-41 molecular sieves have been successfully prepared by a direct synthesis method. The influence of various synthesis conditions such as metal content, times of stirring and hydrothermal treatment of the synthesis gel on the structural and acid properties has been systematically investigated. Although the samples exhibit high structural regularity and surface area values, the same appear to be slightly decreased when a higher amount of aluminum is incorporated. Moreover, while these physical parameters are improved by increasing hydrothermal treatment up to 6 days they are not notably affected by the stirring time of synthesis gel. The NMR and FT-IR results demonstrate that a higher Al content favors the higher incorporation of tetrahedral Al into the framework which, besides, strongly depends on both the hydrothermal synthesis time and the stirring time of gel. Thus, the highest incorporation of aluminum into the framework was achieved for Al-MCM-41 with Si/Al initial molar ratio of 20, where the synthesis gel was stirred for 7 h and then hydrothermal treated during 6 days. The FT-IR analysis reveals that the used synthesis procedure leads to the formation of silanol nests at framework defect sites. The introduction of Al into the framework not only enhanced the density of silanol nests but mainly their acid character. Thus, studies of adsorption and thermodesorption of pyridine followed by FT-IR allow us to identify a very weak Brønsted acidity associated with these nest silanols on Al-MCM-41 materials. A clear linear relationship between the concentration of framework Al and the Brønsted acid silanol density indicates that such acidity are closely related to the incorporation of Al into the mesoporous structure. The acid strength of the SiO—H bonds can probably be modified by an inductive effect of the Al present into structure. Meanwhile, evidences of Lewis acidity can be related, at least mainly, to the presence of extra-framework aluminum oxide species formed during calcination. Rearrangement of CHO was carried out on the Al-MCM-41 catalysts with selectivity to ξ-caprolactam of 100%, in all the cases. A linear relationship between the yield to ξ-caprolactam and the density of weak Brønsted sites (acid nest silanols) has been found. Hence, the catalytic performance mainly depends on the acidity of catalyst; we propose that the nest silanols with very weak Brønsted acidity are the most favorable sites for catalyze the Beckmann rearrangement of the CHO toward ξ-caprolactam. Since the Si—M samples present a negligible activity, we think that the introduction of Al in our materials plays a key role for the performance of the active sites. Finally, the Al-M(20)6-7 sample showed the highest yield to ξ-caprolactam (∼60%) under the mild reaction conditions employed (320 °C and *W*/*F* = 40 g h/mol).

Acknowledgements

CONICET Researchers: G.A.M., S.G.C. and G.A.E. *CONICET Fellowship*: E.G.V. The authors are grateful to CONICET and UTN-FRC for the financial support. The authors also thank J.D. Fernández for assistance with surface area and FT-IR measurements.

References

[1] T. Yanagisawa, T. Shimizu, K. Kuroda, C. Kato, Bull. Chem. Soc. Jpn. 63 (1990) 988–992.
[2] J. Beck, C. Chu, I. Johnson, C. Kresge, M. Leonowicz, W. Roth, J. Vartuli, WO 91/11390, 1991.
[3] C. Kresge, M. Leonowicz, W. Roth, J. Vartuli, J. Beck, Nature 359 (1992) 710–712.
[4] J. Beck, J. Vartuli, W. Roth, M. Leonowicz, C. Kresge, K. Schmidt, C. Chu, D. Olson, E. Sheppard, S. McCullen, J. Higgins, J. Schenkler, J. Am. Chem. Soc. 114 (1992) 10834–10843.
[5] S. Inagaki, Y. Fukushima, K. Kuroda, J. Chem. Soc. Chem. Commun. (1993) 680–682.
[6] J. Vartuli, K. Schmidt, C. Kresge, W. Roth, M. Leonowicz, S. McCullen, S. Hellring, J. Beck, J. Schlenker, D. Olson, E. Sheppard, Chem. Mater. 6 (1994) 2317–2326.
[7] P. Tanev, T. Pinnavaia, Science 271 (1996) 1267–1269.
[8] S. Bagshaw, E. Prouzet, T. Pinnavaia, Science 269 (1995) 1242–1244.
[9] W. Kolodziejski, A. Corma, M. Navarro, J. Perez Pariente, Solid State Nucl. Magn. Reson. 2 (1993) 253–259.
[10] P. Tanev, M. Chibwe, T. Pinnavaia, Nature 368 (1994) 321–323.
[11] R. Schmidt, D. Akporiaye, M. Stocker, O. Ellestad, J. Chem. Soc. Chem. Commun. (1994) 1493–1495.
[12] G. Eimer, L. Pierella, G. Monti, O. Anunziata, Catal. Lett. 78 (2002) 65–75.
[13] G. Eimer, L. Pierella, G. Monti, O. Anunziata, Catal. Commun. 4 (2003) 118–123.
[14] K. Chaudhari, R. Bal, A. Chandwadkar, S. Sivasanker, J. Mol. Catal. A 177 (2002) 247–253.
[15] L. Forni, C. Tosi, G. Fornasari, F. Trifiro, A. Vaccari, J. Nagy, J. Mol. Catal. A 221 (2004) 97–103.
[16] A. Ko, C. Hung, C. Chen, K. Ouyang, Catal. Lett. 71 (2001) 219–224.
[17] D. Zhang, R. Wang, X. Yang, Catal. Commun. 12 (2011) 399–402.
[18] L. Dai, K. Koyama, T. Tatsumi, Catal. Lett. 53 (1998) 211–214.
[19] J. Chang, A. Ko, Catal. Today 97 (2004) 241–247.
[20] R. Maheswari, K. Shanthi, T. Sivakumar, S. Narayanan, Appl. Catal. A 248 (2003) 291–301.
[21] C. Ngamcharussrivichai, P. Wu, T. Tatsumi, Catal. Commun. 8 (2007) 135–138.
[22] T. Conesa, J. Campelo, D. Luna, J. Marinas, A. Romero, Appl. Catal. B 70 (2007) 567–576.
[23] T. Conesa, J. Hidalgo, R. Luque, J. Campelo, A. Romero, Appl. Catal. A 299 (2006) 224–234.
[24] D. Mao, G. Lu, Q. Chen, Appl. Catal. A 279 (2005) 145–153.
[25] D. Mao, G. Lu, Q. Chen, Appl. Catal. A 263 (2004) 83–89.
[26] D. Mao, G. Lu, Q. Chen, Z. Xie, Z. Zhang, Catal. Lett. 77 (2001) 119–124.
[27] B. Xu, S. Cheng, X. Zhang, S. Ying, Q. Zhu, Chem. Commun. (2000) 1121–1122.
[28] L. Forni, G. Fornasari, C. Tosi, F. Trifiro, A. Vaccari, F. Dumeignil, J. Grimblot, Appl. Catal. A 248 (2003) 47–57.
[29] T. Curtin, J.B. McMonagle, B.K. Hodnett, Catal. Lett. 17 (1993) 145–150.
[30] T. Curtin, J.B. McMonagle, B.K. Hodnett, Appl. Catal. A 93 (1992) 91–101.
[31] T. Curtin, J.B. McMonagle, B.K. Hodnett, Appl. Catal. A 93 (1992) 75–89.
[32] G. Heitmann, G. Dahlhoff, W. Holderich, J. Catal. 186 (1999) 12–19.
[33] H. Ichihashi, M. Kitamura, Catal. Today 73 (2002) 23–28.
[34] L. Forni, G. Fornasari, G. Giordano, C. Lucarelli, A. Katovic, F. Trifiro, C. Perri, J. Nagy, Phys. Chem. Chem. Phys. 6 (2004) 1842–1847.
[35] H. Kath, R. Glaser, J. Weitkamp, Chem. Eng. Technol. 24 (2001) 150–153.
[36] C. Flego, L. Dalloro, Microporous Mesoporous Mater. 60 (2003) 263–271.
[37] T. Komatsu, T. Maeda, T. Yashima, Microporous Mesoporous Mater. 35 (2000) 173–180.
[38] M. Camblor, A. Corma, H. Garcia, V. Semmer-Herledan, S. Valencia, J. Catal. 177 (1998) 267–272.
[39] T. Takahashi, T. Kai, E. Nakao, Appl. Catal. A 262 (2004) 137–142.
[40] G. Heitmann, G. Dahlhoff, J. Niederer, W. Holderich, J. Catal. 194 (2000) 122–129.
[41] C.-C. Tsai, C.-Y. Zhong, I. Wang, S.-B. Liu, W.-H. Chen, T.-C. Tsai, Appl. Catal. A 267 (2004) 87–94.
[42] G. Dahlhoff, U. Barsnick, W. Holderich, Appl. Catal. A 210 (2001) 83–95.
[43] P. Singh, R. Bandyopadhyay, S. Hegde, B. Rao, Appl. Catal. A 136 (1996) 249–263.
[44] E. Herrero, O. Anunziata, L. Pierella, O. Orio, Latin Am. Appl. Res. 24 (1994) 195–202.
[45] H. Ichihashi, Sc. Techn. Catal Series Studies in Surface Science and Catalysis, 2002, pp. 73–79.
[46] Y. Izumi, H. Ichihashi, Y. Shimazu, M. Kitamura, H. Sato, Bull. Chem. Soc. Jpn. 80 (7) (2007) 1280–1287.

[47] A. Aucejo, M. Burguet, A. Corma, V. Fornes, Appl. Catal. 22 (1986) 187–200.
[48] T. Curtin, J.B. McMonagle, B.K. Hodnett, Studies in surface science and catalysis, in: M. Guisnet (Ed.), Heterogeneous Catalysis and Fine Chemicals II, vol. 59, Elsevier, Amsterdam, 1991, pp. 531–538.
[49] L. Dai, R. Hayasaka, Y. Iwaki, K.A. Koyano, T. Tatsumi, Chem. Commun. (1996) 1071–1072.
[50] T. Yashima, K. Miura, T. Komatsu, Stud. Surf. Sci. Catal. 84 (1994) 1897–1904.
[51] H. Sato, K. Hirose, M. Kitamura, Y. Nakamura, Stud. Surf. Sci. Catal. 49 (1989) 1213–1222.
[52] G. Heitmann, G. Dahlhoff, W. Holderich, Appl. Catal. A 185 (1999) 99–108.
[53] P. O'Sullivan, L. Forni, B.K. Hadnett, Ind. Eng. Chem. Res. 40 (2001) 1471–1475.
[54] W. Hölderich, J. Röseler, G. Heitmann, A. Liebens, Catal. Today 37 (1997) 353–366.
[55] H. Sato, S. Hasabe, H. Sakurai, K. Urabe, Y. Izumi, Appl. Catal. 29 (1987) 107–115.
[56] T. Ushikubo, K. Wada, J. Catal. 148 (1994) 138–148.
[57] V. Elías, M. Crivello, E. Herrero, S. Casuscelli, G. Eimer, Ind. Eng. Chem. Res. 48 (2009) 9076–9082.
[58] G. Eimer, L. Pierella, O. Anunziata, Series Stud. Surf. Sci. Catal. 135 (2001) 377–397.
[59] L. Cedeño, D. Hernandez, T. Klimova, Ramirez, Appl. Catal. A 241 (2003) 39–50.
[60] D. Ma, F. Deng, R. Fu, X. Han, X. Bao, J. Phys. Chem. B 105 (9) (2001) 1770–1779.
[61] G. Eimer, S. Casuscelli, G. Ghione, M. Crivello, E. Herrero, Appl. Catal. A 298 (2006) 232–242.
[62] A. Palani, N. Gokulakrishnan, M. Palanichamy, A. Pandurangan, Appl. Catal. A 304 (2006) 152–158.
[63] M. Boccuti, K. Rao, A. Zecchina, G. Leofanti, G. Petrini, Stud. Surf. Sci. Catal. 48 (1989) 133–144.
[64] A. Thangaraj, R. Kumar, S. Mirajkar, P. Ratnasamy, J. Catal. 130 (1991) 1–7.
[65] K. Li, C. Lin, Catal. Today 97 (2004) 257–261.
[66] A. Corma, Chem. Rev. 97 (1997) 2373–2419.
[67] M. Selvaraj, A. Pandurangan, K.S. Seshadri, P.K. Sinha, K.B. Lal, Appl. Catal. A 242 (2003) 264–347.
[68] D. Zhang, R. Wang, X. Yang, W. Yao, React. Kinet. Mech. Cat. 101 (2010) 455–460.
[69] A. Jentys, K. Kleestorfer, H. Vinek, Microporous Mesoporous Mater. 27 (1999) 321–328.
[70] B. Chakraborty, B. Viswanathan, Catal. Today 49 (1999) 253–260.
[71] V. Zholobenko, D. Plant, A. Evans, S. Holmes, Microporous Mesoporous Mater. 44–45 (2001) 793–799.
[72] G. Eimer, S. Casuscelli, C. Chanquia, V. Elías, M. Crivello, E. Herrero, Catal. Today 133 (2008) 639–646.
[73] C. Chanquía, L. Andrini, J. Fernández, M. Crivello, F. Requejo, E. Herrero, G. Eimer, J. Phys. Chem. C 114 (2010) 12221–12229.
[74] D. Trong On, S. Nguyen, V. Hulea, E. Dumitriu, S. Kaliaguine, Microporous Mesoporous Mater. 57 (2003) 169–180.
[75] D. Srinivas, R. Srivastava, P. Ratnasamy, Catal. Today 96 (2004) 127–133.
[76] A. Sakthivel, S. Dapurkar, N. Gupta, S. Kulshreshtha, P. Selvam, Microporous Mesoporous Mater. 65 (2003) 177–187.
[77] R. Mokaya, W. Jones, Z. Luan, M. Alba, J. Klinowski, Catal. Lett. 37 (1996) 113–120.
[78] C. Otero Arean, M. Rodriguez Delgado, V. Montouillout, J. Lavalley, C. Fernandez, J. Cuart Pascual, J. Parra, Microporous Mesoporous Mater. 67 (2004) 259–264.
[79] G. Turnes Palomino, J. Cuart Pascual, M. Rodrıguez Delgado, J. Bernardo Parra, C. Otero Arean, Mater. Chem. Phys. 85 (2004) 145–148.
[80] K. Góra-Marek, M. Derewinski, P. Sarv, J. Datka, Catal. Today 101 (2005) 131–138.
[81] C. Morterra, G. Magnacca, Catal. Today 27 (1996) 497–532.
[82] A. Katovic, G. Giordano, B. Bonelli, B. Onica, E. Garrone, P. Lentz, J. Nagy, Microporous Mesoporous Mater. 44–45 (2001) 275–281.
[83] E. Escalona Platero, M. Peñarroya Mentruit, C. Otero Arean, A. Zecchina, J. Catal. 162 (1996) 268–276.
[84] L. Chen, L. Noreña, J. Navarrete, J. Wang, Mater. Chem. Phys. 97 (2006) 236–242.
[85] J. Anderson, C. Fergusson, I. Rodríguez-Ramos, A. Guerrero-Ruiz, J. Catal. 192 (2000) 344–354.
[86] M. Coles, R. Jordan, J. Am. Chem. Soc. 119 (1997) 8125.